Journal of Electroceramics 4:2/3, 299–303, 2000
© 2000 Kluwer Academic Publishers. Manufactured in The Netherlands.

Crystallographic Orientation Dependence of the Schottky Properties of Au/$SrTiO_3$ Junctions

TAKASHI SHIMIZU, YUJI USUI,* TOMOYUKI NAKAGAWA* & HIDEYO OKUSHI
Electrotechnical Laboratory, 1-1-4 Umezono, Tsukuba, Ibaraki 305 Japan

Abstract. Crystallographic orientation dependence of the Schottky properties of Au/Nb-doped $SrTiO_3$ (STO:Nb) junctions has been investigated using single crystals of STO:Nb (1 0 0) and (1 1 1). It is found from electrical properties that the Schottky barrier height (SBH) of the Au/STO:Nb junctions estimated from current density (*J*)-voltage (*V*) characteristics shows crystallographic orientation dependence, while the flat band voltage estimated from capacitance (*C*)-voltage (*V*) characteristics is independent of the orientation. Displacement currents originated from the junction capacitance have been clearly observed at reverse bias voltage even in a condition of $|dV/dt| \geq 8.75 \times 10^{-3}$ [V/s] because of large electrostatic permittivity of the STO, and the displacement currents also showed crystallographic orientation dependence. The different response in the electrical properties of the Schottky junctions suggests that electric properties of intrinsic low permittivity layers, which exist at Au/STO:Nb interfaces, have the crystallographic orientation dependence.

Keywords: metal/oxide interface, Schottky junction, chrystallographic orientation dependence, ozone surface treatment, intrinsic low permittivity layer

1. Introduction

Surface and interface of metal-oxides play important roles in a wide range of physical and chemical phenomena [1]. Recent progress of oxide thin film technology for future application of dielectric or ferroelectric oxides to Si ultra-large-scale-integration (ULSI) devices has attracted much attention to the role of metal/oxide interfaces [2]. Metal/$SrTiO_3$ (STO) interface is one of the most important metal/oxide interfaces, since the STO is one of the attractive transition-metal oxides as a photo-catalyst [3], a dielectric with large electrostatic permittivity [4] and an oxide superconductor [5]. Using single crystals of TiO_2 and STO, we have recently proved that a suitable surface treatment for oxides improved drastically the metal/oxide junction properties [6] and have succeeded in investigating intrinsic properties of metal/Nb-doped $SrTiO_3$ (STO:Nb) (1 0 0) Schottky junctions [7]. In the previous study of the metal/STO:Nb (1 0 0) Schottky junctions, it was found that there exists an intrinsic low permittivity layer (ILP) at very interface of the metal/STO:Nb (1 0 0) Schottky junctions [7] even in a case of Au/STO:Nb (1 0 0) junctions. Since crystallographic orientation dependence of surface and interface properties of single crystals is also important in many physical and chemical aspects [8,9], it is also informative to clear out crystallographic orientation dependence of the Schottky properties of metal/STO:Nb junctions. In this paper, we have studied the crystallographic orientation dependence of the Schottky properties of the Au/STO:Nb junctions using single crystals of STO:Nb (1 0 0), (1 1 1) and (1 1 0) with the suitable surface treatment of oxides developed before [7]. We found that the Schottky barrier height (SBH) of the Au/STO:Nb junctions estimated from current density (*J*)-voltage (*V*) characteristics show crystallographic orientation dependence, while the flat band voltage (V_{flat}) estimated from capacitance (*C*)-voltage (*V*) characteristics is independent of the orientation. Origin of the different response in the electrical

*On leave from Chuo University.

properties of the Schottky junctions is discussed from different electrical properties of the ILP layer [7] of the STO with considering origins of its crystallographic orientation dependence.

2. Experimental

Verneuil grown single crystal substrates of STO (1 0 0) and (1 1 1) doped with Nb at 0.01 wt.% were used as specimens. As-received substrates of the STO:Nb (1 0 0) which was chemically etched by buffered HF acid to have TiO_2 terminated flat terraces and have steps being 0.4 nm high was annealed in flowing O_2 at 1000°C for 1 h and 500°C for 4 h to obtain atomically flat terraces and well-ordered steps [7,10]. The annealed substrate, mounted on a INCONEL holder, was heated up to 500°C for 20 min in a high-purity ozone atmosphere of around 1×10^{-3} Pa to eliminate carbon contamination in a ultra-high vacuum chamber without introducing oxygen deficiencies of the substrate during annealing. After the temperature of the holder was cooled down below 110°C, 99.99% pure gold was deposited in-situ through a stain-less steel pattern of holes to form Schottky junctions of 200 μm in diameter. After about 0.01 nm/s for initial 16 nm deposition, the deposition rate of Au was increased about 0.03 nm/s to form 80 nm-thick electrodes. Detailed experimental procedure has been described elsewhere [7]. Substrates of STO:Nb (1 1 1) without buffered HF etching were annealed in flowing O_2 at 1000°C for 1 h and at 500°C for 4 h, and were performed the high-purity ozone surface treatment in the vacuum chamber.[1] When the temperature of the holder was cooled to 110°C, the gold was deposited in-situ through the mask pattern. The deposition rate was about 0.01 nm/s for initial 35 nm and about 0.03 nm/s to become 80 nm thick. The *J-V* and *C-V* characteristics were measured using a picoampere meter and an impedance analyzer. Displacement currents were also measured using the picoampere meter, applying voltage triangles with a function generator, to investigate dielectric properties of the junctions under low-frequency conditions. Applied voltages were typically between -3.2 V and $+0.5$ V during the measurements of the displacement currents.

3. Results and Discussion

A typical *J-V* characteristic of Au/STO:Nb (1 1 1) junctions compared with that of Au/STO:Nb (1 0 0) is shown in Fig. 1. Reverse bias leak currents were lower than 5×10^{-9} A/cm^2 and rectification ratio of ± 1.5 eV is over nine order of magnitude for both junctions, which guaranteed the effectiveness of the high-purity ozone surface treatment for oxides reported before [7]. The ideality factors of the junctions were estimated to be 1.30 for the (1 1 1) junction and 1.15 for the (1 0 0) junction, respectively. The larger current density of the (1 1 1) junction at the same applied voltage indicates that the SBH

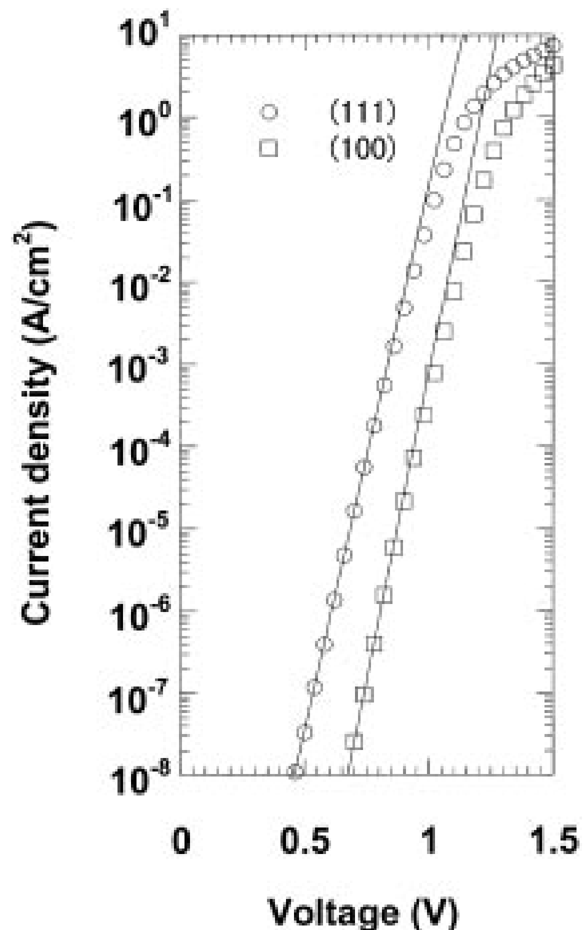

Fig. 1. Crystallographic orientation dependence of *J-V* characteristics of Au/STO:Nb junctions. Measurement temperatures are 294 K for the (1 1 1) junction and 292 K for the (1 0 0) junction, respectively.

of the (1 1 1) junction is lower than that of the (1 0 0) junction. Using thermionic-emission theory and assuming the Richardson constant $A^* = 156\,\text{A/cm}^2\text{K}^2$, the SBH of the (1 1 1) junction is estimated to be 1.24 eV, which is about 0.2 eV lower than that of (1 0 0) junction of 1.46 eV.

Figure 2 (a) and (b) show C^{-2}-V characteristics of (1 1 1) and (1 0 0) junctions, respectively. Measurement frequencies are 0.1 K, 1 K, 10 K, 100 K, 500 K. All the C^{-2} in a range between 0 and -3 V seems to have almost linear correlation to applied reverse bias voltages at room temperature, while detailed analyses of the C^{-2} have actually shown nonlineality reflecting the field-dependent permittivity of the STO [7]. For simplicity, flat band voltages (▽flat) for both junctions were estimated from intercepts on voltage axes using linear fittings of C^{-2}-V plots as in the case of Schottky junctions of conventional semiconductors. The estimated V_{flat} of 1.74 V for the (1 1 1) junction and of 1.76 V for the (1 0 0) junction are almost the same. This is in contrast to the SBH estimated from the J-V results. It is noted that while C^{-2}-V characteristics of the (1 0 0) junction shown in the Fig. 2(b) were almost independent of measurement frequencies, the C^{-2}-V characteristics of the (1 1 1) junction in the Fig. 2(a) show clear frequency dependence. It is still unknown whether the frequency dependence is due to interface properties of the junctions or bulk properties of the substrates such as existence of deep levels in the (1 1 1) substrates, since several (1 0 0) junctions also showed such frequency dependent C^{-2}-V characteristics.

Because of large junction capacitances compared with those in the Schottky junctions of conventional semiconductors, we have investigated displacement currents of the junctions and studied their crystallographic orientation dependence applying voltage triangles under predominantly reverse bias condition. Displacement currents were clearly observed in both Schottky junctions even for $|dV/dt| \leq 8.75 \times 10^{-3}$ volt/sec because of large junction capacitances due to the large permittivity of the STO. As shown in Fig. 3 where we use voltage triangles $|dV/dt| = 8.70 \times 10^{-2}$ volt/sec for the (1 1 1) junction and $|dV/dt| = 9.86 \times 10^{-2}$ volt/sec for the (1 0 0) junction, absolute value of the displacement current $|dQ/dt|$ decreases when the reverse bias voltage increases, and the dQ/dt increases when the reverse bias voltage decreases. This result is consistent with variation of depletion width W in the reverse bias

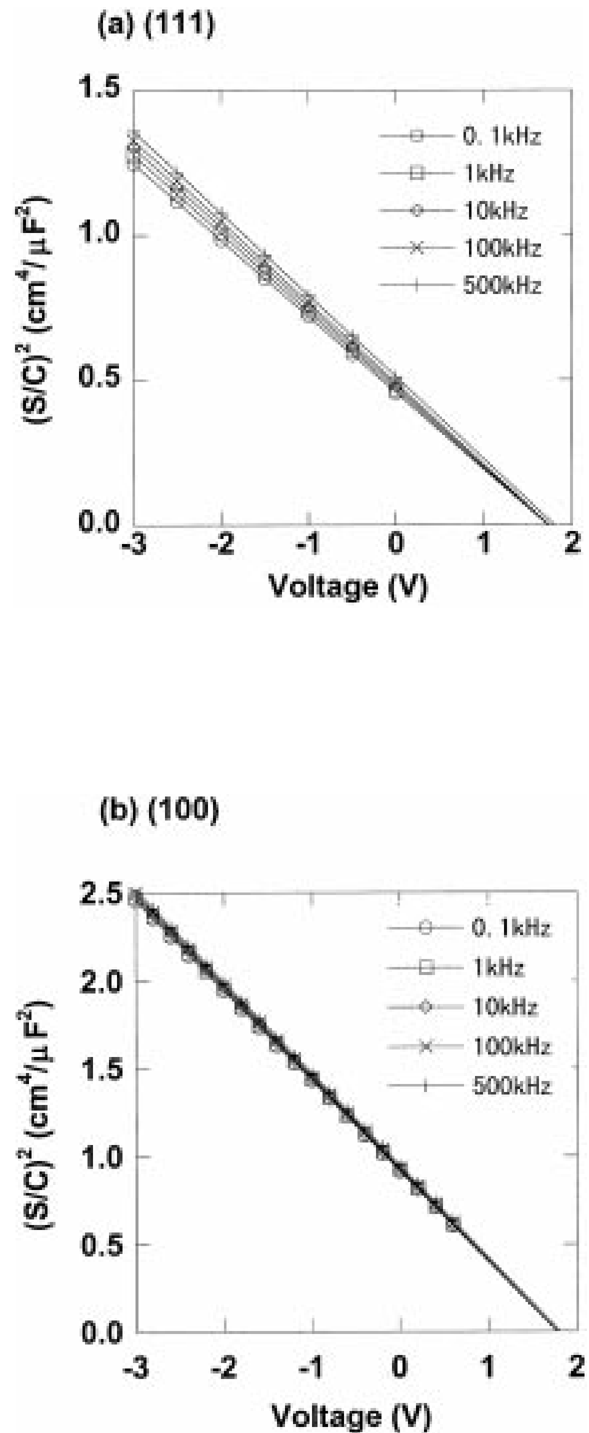

Fig. 2. Crystallographic orientation dependence of $C^{-2} - V$ characteristics of Au/STO:Nb junctions. Measurement temperatures are 294 K for the (1 1 1) junction and 292 K for the (1 0 0) junction, respectively.

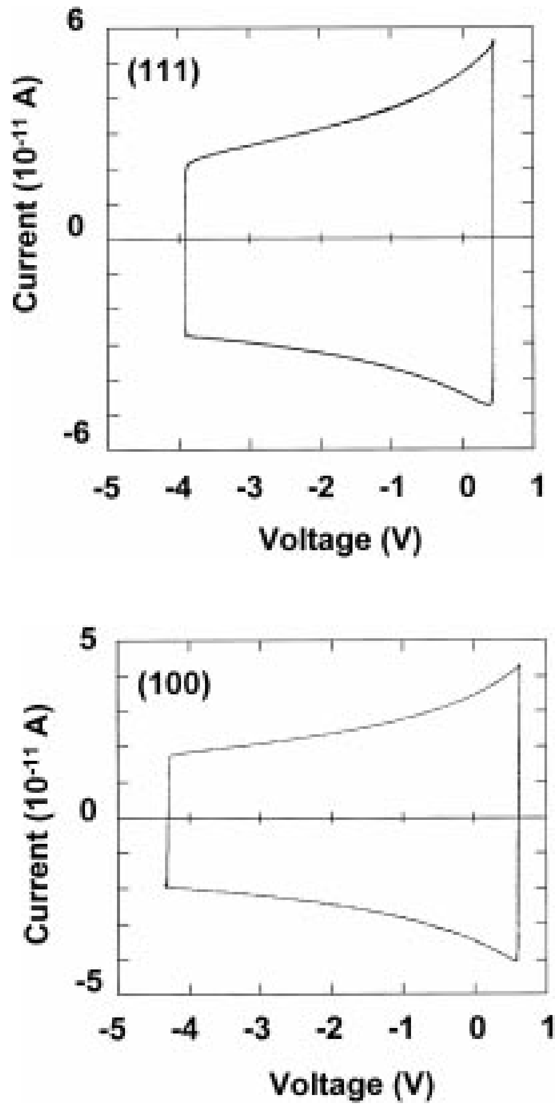

Fig. 3. Displacement currents of Au/STO:Nb (1 1 1) and Au/STO:Nb (1 0 0) junctions. Measurement temperatures are 294 K for the (1 1 1) junction and 292 K for the (1 0 0) junction, and a measurement frequency is 0.01 Hz for both junctions. The $|dV/dt| = 8.70 \times 10^{-2}$ V/s for the (1 1 1) junction and $|dV/dt| = 9.86 \times 10^{-2}$ V/s for the (1 0 0) junction, respectively. Both junctions have 3.14×10^{-4} cm^2 junction area.

condition, since $|dQ/dt| = |d(N_d W)/dt| = N_d |dW/dV||dV/dt|$ where N_d is space charge density in the depletion region. It is noted from the result that when conduction current is low enough, especially in the reverse bias condition, a component of the displacement current has not been ignored in the *J-V* characteristics of the junctions since the component of the displacement current is always included beside with the conduction current.

In case of the (1 0 0) junction, almost symmetric displacement currents were observed, which indicates symmetric variation of depletion width in the applied voltage triangles. This symmetric displacement current guarantees that the *C-V* characteristics are independent of measuring directions of the applied bias voltage, which means that significant deep levels or interface states are absent in the (1 0 0) junction. Therefore the symmetric displacement current shown in the Fig. 3(b) is consistent with the results shown in Fig. 2(b) observing independent C^{-2} of measurement frequencies. Displacement currents of the (1 1 1) junction were rather asymmetric, which suggests existence of interface states and/or deep levels in the (1 1 1) junction. This result is also consistent with the frequency-dependent C^{-2}-V characteristics shown in the Fig. 2(a). It is noted that analytical summation of positive and negative displacement currents at the same reverse bias voltage suggests the existence of electron-trap states near the interface. Origin of the asymmetric displacement current is still unclear yet because the field-dependent permittivity of the STO and the ILP layer at the interface make it difficult to determine the origin using conventional transient capacitance methods of the junction.

Discrepancy between the SBH results from the *J-V* characteristics and V_{flat} results from the C^{-2}-V characteristics is probably originated from crystallographic orientation dependence of the ILP layer at the Au/STO:Nb interface, the existence of which was recently proved by temperature dependence of the electrical properties of the Au/STO:Nb (1 0 0) junctions [7]. Schematic band diagram of the metal/STO:Nb junction with the ILP layer is shown in Fig. 4. When the ILP layer exists at the interface, the SBH from the *J-V* characteristics and the flat band voltage from the *C-V* characteristics are estimated to be different, since the SBH strongly depends on dielectric properties of the ILP layer, while the flat band voltage is rather insensitive to the properties of the ILP layer. Therefore, if the dielectric properties of the ILP layer has crystallographic orientation dependence, the crystallographic orientation dependence of the SBH from the *J-V* results shown in the Fig. 1 is reasonable even when bulk (1 0 0) and (1 1 1) STO substrates have the same minimum energy position of the conduction band of the bulk STO and

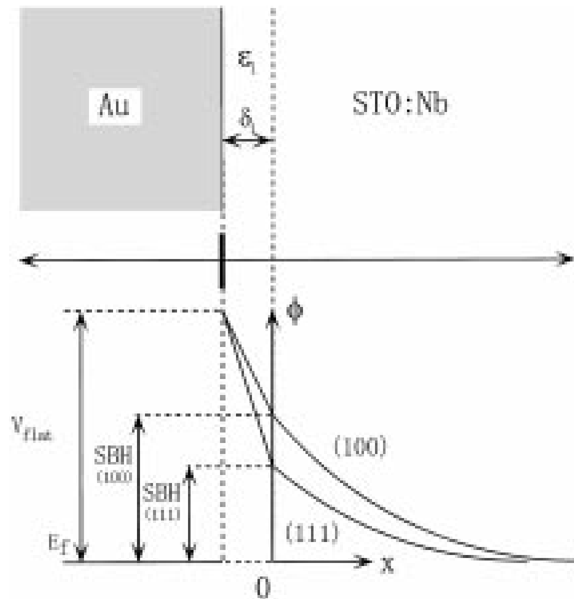

Fig. 4. Schematic band diagram for a Au/STO:Nb junction. Symbols ε_i and δ_i denote electrostatic permittivity and thickness of an intrinsic low permittivity layer at interface. Symbols E_f, V_{flat} and SBH denote the fermi energy of Au, the flat band voltage and the Schottky barrier height, respectively.

have the same electrostatic permittivity in the depletion region of the STO. Although actual origin of the ILP layer is still unclear yet, it is reasonable the ILP layer has such crystallographic orientation dependence because atomic configurations, atomic rearrangements, reconstruction and reactivities of the STO surfaces are different.[2] The crystallographic orientation dependence of the dielectric properties of the ILP layer is also consistent with reported results of non-doped STO thin film capacitors by Komatsu and Abe [11]. They have prepared (1 0 0) and (1 1 0) oriented epitaxial STO thin films by rf sputtering and pointed out that interface energy between metal electrodes and STO films is essential to the dielectric properties of STO film capacitors. Our preliminary results of (1 1 0) junctions also supported different electrical response of the ILP layer of the (1 1 0) junction from that of the (1 0 0) junction. Further study with more careful preparations in forming metal/STO:Nb junctions is necessary to clarify precise crystallographic orientation dependence of the electric properties of the metal/STO:Nb junctions including density of the interface states and the deep levels of the STO, quantitatively.

4. Summary

Crystallographic orientation dependence of the Schottky properties of Au/STO:Nb junctions has been investigated using single crystals of STO:Nb (1 0 0) and (1 1 1). The SBH from *J-V* characteristics shows crystallographic orientation dependence, while the flat band voltage from *C-V* characteristics is independent of the orientation. Displacement currents originated from the junction capacitance have been clearly observed at reverse bias voltage even in a condition of $|dV/dt| \geq 8.75 \times 10^{-3}$ [V/s], and the displacement currents also showed crystallographic orientation dependence. The different response in the electrical properties suggests that the intrinsic low permittivity layer at the Au/STO:Nb interface has crystallographic orientation dependence.

Notes

1. It is noted that although atomic force microscopy (AFM) images of the (1 1 1) and (1 1 0) substrates show flat surface morphologies, the images were found to be almost featureless even after the 1000°C O_2 annealing. This suggest that surface migration time of the (1 1 1) and (1 1 0) substrates under the annealing condition is still insufficient to form well-ordered surface steps compared with that of the (1 0 0) substrates under the same condition.
2. In fact, doping dependency of the SBH, which is observed in the (1 0 0) junctions, should also be considered when precise crystallographic orientation dependence of the SBH is investigated. The doping dependency of the SBH will also be studied in detail in the near future.

References

1. V.E. Henrich and P.A. Cox, *The Surface Science of Metal Oxides*. (Cambridge University Press, New York, 1994).
2. Y. Shimamoto, K. Kushida-Abdelghafer, H. Miki, and Y. Fujisaki, *Appl. Phys. Lett.*, **70**, 70 (1997).
3. J.G. Mavroides, J.A. Kafalas, and D.F. Kolesar, *Appl. Phys. Lett.*, **28**, 241 (1976).
4. D.E. Grupp and A.M. Goldman, *Science*, **276**, 392 (1997).
5. J.F. Schooley, W.R. Hosler, and M.L. Cohen, *Phys. Rev. Lett.*, **12**, 474 (1964).
6. T. Shimizu and H. Okushi, *Appl. Phys. Lett.*, **67**, 1411 (1995).
7. T. Shimizu and H. Okushi, *J. Appl. Phys.*, **85**, 7244 (1999).
8. R.T. Tung and J.M. Gibson, *J. Vac. Sci. Technol.*, **A3**, 987 (1985).
9. D.R. Strongin, J. Carrazza, S.R. Bare, and G.A. Somorjai, *J. Catal.*, **103**, 213 (1987).
10. T. Shimizu, N. Gotoh, N. Shinozaki, and H. Okushi, *Appl. Surf. Sci.*, **117/118**, 400 (1997).
11. S. Komatsu and K. Abe, *Jpn. J. Appl. Phys.*, **34**, 3597 (1995).